Cyclic Biamperometry

by

Mohammad Mehdi Rahimi

A thesis
presented to the University of Waterloo
in fulfillment of the
thesis requirement for the degree of
Master of Science
in
Chemistry

Waterloo, Ontario, Canada, 2009

I hereby declare that I am the sole author of this thesis. This is a true copy of the thesis, including any required final revisions, as accepted by my examiners.

I understand that my thesis may be made electronically available to the public.

Abstract

In this thesis, cyclic biamperometry (CB) as a new method in electrochemistry, has been introduced and investigated. The hallmark of this method is the absence of a reference electrode which potentially allows simplification and miniaturization of the measurement apparatus. Similarities and differences of this method and cyclic voltammetry (CV) have been studied and it was shown that under conditions of using standard electrodes, CB has a better sensitivity and a lower detection limit than CV. A new equivalent circuit model for the cell has been proposed and parameters affecting the sensitivity of CB, such as keeping the concentration of one redox species in excess and having a larger W_2 electrode, have been described. The redox cycling effect in biamperometric systems has been investigated and it is shown that improvements of at least two orders of magnitude in sensitivity can be achieved by using interdigitated electrodes (IDEs). In addition, an example for applications of this method, including biamperometric dead-stop titration of 1-naphthol with ferricyanide, has been presented and possible fields in which CB can be incorporated (e.g. monitoring the activity of alkaline phosphatase) have been illustrated. Finally, a few suggestions for future studies and further improvements have been outlined.

Acknowledgements

I would like to thank Prof. Susan Mikkelsen, my supervisor, for her valuable help, guideline, support and patience without which creation of this thesis would be impossible. I would also like to appreciate the financial support provided by NSERC during the course of this project.

Dedication

Dedicated to my parents, brothers and sisters whose love, support and encouragement have given me strength and inspired me in my life.

Contents

List of Tables

List of Figures

List of Abbreviations

ν	Scan rate
A	electroactive surface area
C_{dl}	Capacitance of the double layer
D	Diffusion coefficient
d	distance
E	Potential
$E^{\circ'}$	Formal potential
E_{pa}	Anodic peak potential
E_{pc}	Cathodic peak potential
F	Faraday constant
i	Current
i_p	Peak current
i_{pa}	Anodic peak current
i_{pc}	Cathodic peak current
n	Number of electrons transfered
t	time
V	Voltage
W	Working electrode
Z	Impedance
CB	Cyclic Biamperometry
CV	Cyclic Voltammetry

LSV	Linear Sweep Voltammetry
O	Oxidized form of an species
R	Reduced form of an species

Chapter 1

Introduction

In today's market, accurate, fast and in situ identification and quantitation of various chemical and biochemical analytes is in ever-increasing demand and electrochemistry, as a powerful tool of analytical science, has drawn the attention of researchers for decades. One of the ultimate goals of applied electrochemistry is to construct miniaturized devices with faster responses, lower detection limits and higher sensitivities. This has made chemists not only improve the existing tools but also discover new methods.

Among the various electrochemical methods, amperometry is the most widely used electrochemical method for detection of trace analytes. The method is based on measurement of the current produced at a working electrode in response to an applied potential.

In conventional amperometric methods such as cyclic voltammetry, the potential of the electrode at which the reaction of interest occurs, the working electrode, must be controlled against a reference electrode which draws essentially no current and the absolute potential of which remains constant during the course of the reaction. [1] Although use of a reference electrode is a must in virtually all electrochemical methods, the restrictions of miniaturizing it has been an obstacle for developing the lab-on-chip idea in electrochemistry.

The scope of this thesis is to introduce a new amperometric method which does not require any reference electrode in its circuitry. Lack of a reference electrode and simplicity of the electronic requirements ease the way for automating and arraying the whole apparati involved in such measurements.

1.1 Potential Sweep Methods

In electrochemistry, the behavior of a redox reaction is frequently observed by monitoring a current-time curve at different applied potentials. However, it is not easy to get useful information about the presence of different analytes based on $i-t$

curves alone. Several $i-t$ curves at very closely spaced potentials (e.g. 1 mV) are required.[1]

Usually, more information is obtained when the potential is linearly swept with respect to time, at different rates. In such experiments, the current is recorded as a function of potential which is analogous to recording the current versus time. This method is referred to as linear sweep voltammetry (LSV). In linear sweep voltammetry, for a solution containing an oxidized analyte, the starting potential is usually set well positive of the formal potential of the redox couple ($E^{\circ'}$) for the reduction of the analyte so that only non-faradaic current[1] flows in order to establish a baseline charging current. When the potential of the electrode approaches the $E^{\circ'}$ from the positive direction, the current flows as the reduction proceeds. As the potential passes the $E^{\circ'}$ value, the surface concentration of the analyte reaches zero and mass transfer toward the electrode reaches a maximum rate and then it decreases as the area surrounding the electrode is depleted of the analyte. This phenomenon is observed as a peak, the magnitude of which is proportional to the concentration of the analyte in the solution.[1]

1.1.1 Cyclic Voltammetry

Cyclic voltammetry is an electrochemical method in which the applied potential is swept between two values of V_1 and V_2 at a fixed rate. Here, when the potential V_2 is reached, the scan direction is reversed and the voltage is swept back to V_1. During the scan, the current is measured in an unstirred electrolyte.[2]

The potentials at which reversals take place are called switching potentials. The switching potentials are chosen for a given experiment based on the formal potential of the redox couple. The formal electrode potential of the O/R couple, $E^{\circ'}$ can be measured as the midpoint potential between the two peaks, and gives a value versus the employed reference electrode, which is commonly either Ag/AgCl or a saturated calomel electrode (SCE, Hg/Hg_2Cl_2).

$$E^{\circ'} = \frac{E_{pa} + E_{pc}}{2} \tag{1.1}$$

The important parameters in cyclic voltammetry are the cathodic peak potential, E_{pc}, the anodic peak potential, E_{pa}, the cathodic peak current, i_{pc} and the anodic peak current, i_{pa}. (Figure 1.1)

In cyclic voltammetry, the peak currents are measured by extending the charging current baseline (shown by dashed line in Figure 1.1) and measuring the maximum height of the line segment drawn vertically from the curve to the baseline and the peak potentials are potential values at which peak currents appear.

[1] Non-faradaic or charging current is the current resulting from the accumulation of charges at the electrode-solution interface.

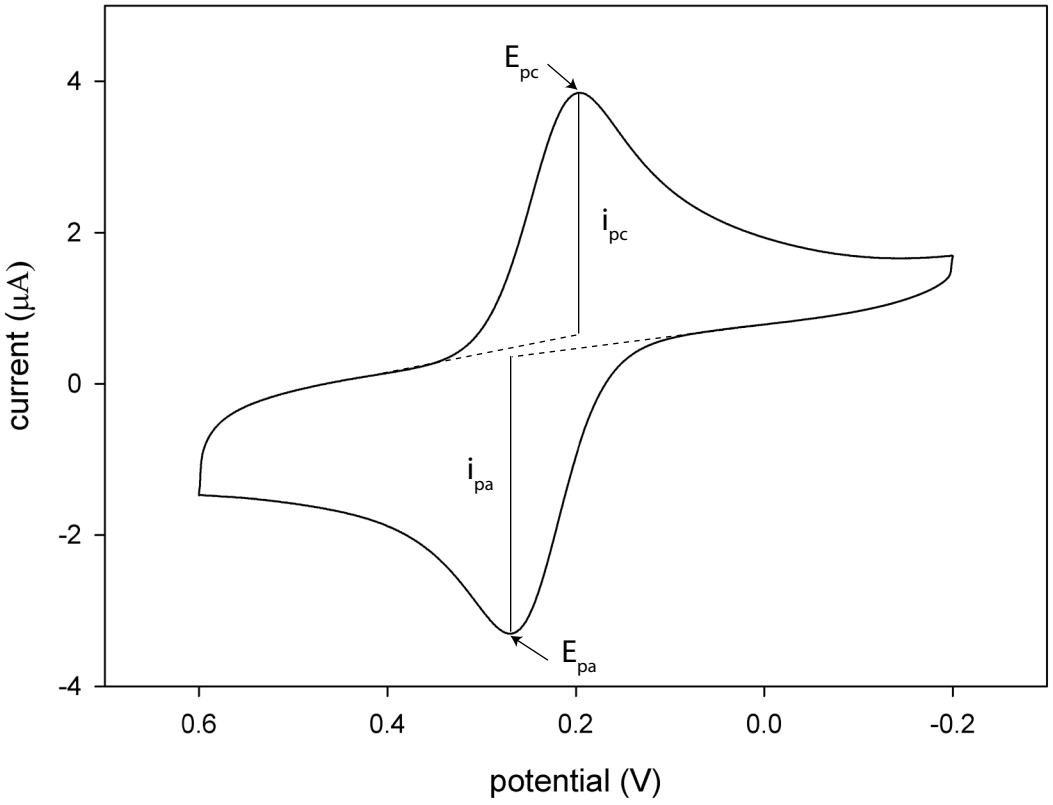

Figure 1.1: Schematic representation of a cyclic voltammogram

For a reversible system, anodic and cathodic peak currents are equal in absolute value but opposite in sign and the difference in peak potentials is $0.0592/n$ where n is the number of electrons involved in the half reaction.[2]

The absolute value of the peak current i_p is defined by the Randles-Sevcik equation,

$$i_p = (2.69 \times 10^5) n^{3/2} A D^{1/2} C \nu^{1/2} \,, \tag{1.2}$$

which applies at 25°C where n is the number of electrons transferred, A is the electroactive surface area in cm^2, D is the diffusion coefficient of the species being oxidized/reduced in cm^2/s, C is the concentration of the analyte in the bulk solution in $\mathrm{mol}/\mathrm{cm}^3$ and ν is the scan rate in V/s.

The peak potential is defined by

$$E_p = E^{\circ'} - 0.029/n \,, \tag{1.3}$$

where E_p and $E^{\circ'}$ are expressed in volts and assumes that the diffusion coefficient of both redox species are the same ($D_O = D_R$) This equation shows that the potential at which the peak occurs, for a reversible system, does not depend on the scan rate.

Another important aspect of voltammetry is the background current which is

the current obtained on a solution containing all components except the electroactive analyte of interest. Background current is composed of (i) residual current, oxidation or reduction of other species in the solution e.g. dissolved oxygen and (ii) charging current which is the non-faradaic current required to charge the electrode to a certain potential (analogous to charging a capacitor). Therefore, the peak current must be measured in a manner to exclude the background current. A common method is to extrapolate baseline current that precedes the faradaic current and measure i_p by difference.[1]

The charging current is directly proportional to the scan rate as given by the following equation

$$i_c = C\frac{dE}{dt} = AC_{dl}\nu\,, \tag{1.4}$$

where A is the electroactive surface area in cm^2 and C_{dl} is the capacitance of the double layer in faradays per square centimeter.

The signal from cyclic voltammetry can be improved by increasing the scan rate, which increases the i_p; however, at higher scan rates charging current becomes a problem because i_c increases faster with ν compared to i_p ($i_c \propto \nu$, $i_p \propto \nu^{1/2}$).

1.1.2 Biamperometry

Biamperometry involves the application of a small constant voltage (e.g. 100 mV) across two polarizable electrodes (usually with approximately equal surface areas) in an electrolyte solution containing redox-active species. As a result of the applied voltage, when both halves of a redox couple are present in solution, a current is produced which is proportional to the concentration of the limiting species.

Biamperometry is a relatively old electrochemical method introduced more than 90 years ago to indicate endpoints in coulometric titrations.[3] Since then, the method has been applied to the detection of redox-active chemicals [4–6] and more recently, it has been integrated into an electrochemical detection system in flow injection analysis and biosensors.[7–10]

In a few recent studies, biamperometry has been used with different redox reactions of closely matched potential values for each half reaction [11–13]. Also, scanning biamperometry was introduced recently in order to determine an appropriate fixed potential for biamperometric measurements in flowing solutions, using interdigitated electrodes.[10,14,15] In these studies [10,14,15], the redox cycling effect at closely-spaced interdigitated electrodes and the effect of the small diffusion layers at the electrodes, which facilitates renewal of the reactant and removal of the products at the electrode surfaces, trigger sigmoid plots of current versus applied voltage. These sigmoid plots have been believed to be the normal shape of biamperometric voltammograms at interdigitated electrodes. However, under quiet solution conditions, responses similar to distorted voltammograms have also been reported.[16]

Although all of these analytical applications are apparently successful under the stated conditions, the fundamental differences between biamperometric and standard amperometric methods are not clear. In this thesis, cyclic biamperometry (CB),a new method in electroanalytical chemistry, is investigated.

Cyclic Biamperometry

Cyclic biamperometry deals with the measurement of current as a function of an applied triangular voltage waveform across two polarizable electrodes in an aqueous medium. In this method, the voltage applied across the electrode-solution interface is linearly scanned from an initial value V_i to a final voltage V_f and again back to V_i at a constant rate. The start point is normally chosen far from the formal potential of the electroactive couple on one side (e.g. +400 mV) where neither of the redox species can undergo electrolysis and hence there is no faradaic current. Then the voltage is scanned at constant rate until it reaches the final value (e.g. -400 mV), at which point the scan direction is reversed. As the voltage is swept, both reduction and oxidation occur at the opposite electrodes, and this results in the faradaic current flow.

A biamperogram is very similar to a voltammogram with respect to the general shape, but the graph is centered at the origin of both current and potential. Like CV, the important parameters in cyclic biamperometry are peak potential, E_p, and peak current ,i_p, which are defined a similar way. (Figure 1.2)

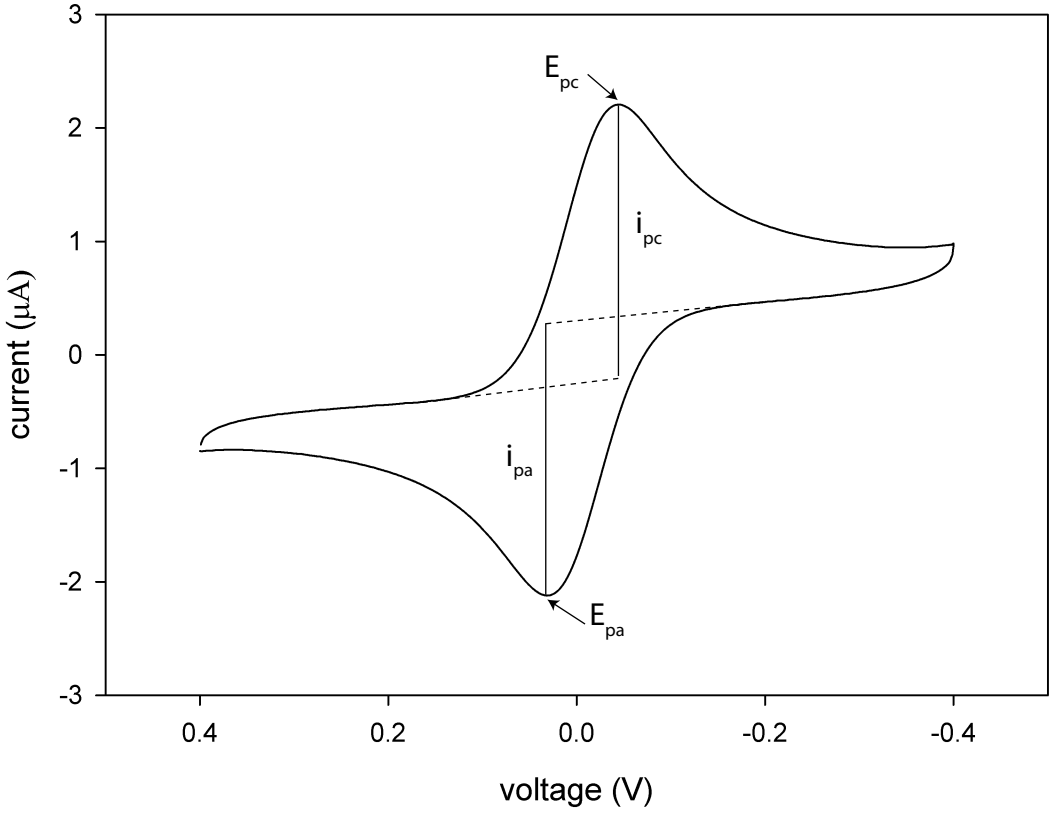

Figure 1.2: Schematic representation of cyclic biamperometry

1.1.3 Interdigitated Electrodes and Redox Cycling

IDEs consist of a set of closely and alternately positioned anodes and cathodes. The potentials of cathodes and anodes can be independently controlled. Upon fixing the potentials of the two working electrodes, oxidation of analyte can occur on the surface of anodes while the reduction of the corresponding species occurs on the surface of the cathodes. Since each analyte, ideally, can undergo multiple redox cycles, signal amplification can occur by redox-cycling, resulting in multiple electrons, and enhanced currents, for any given analyte concentration. (Figure 1.3)

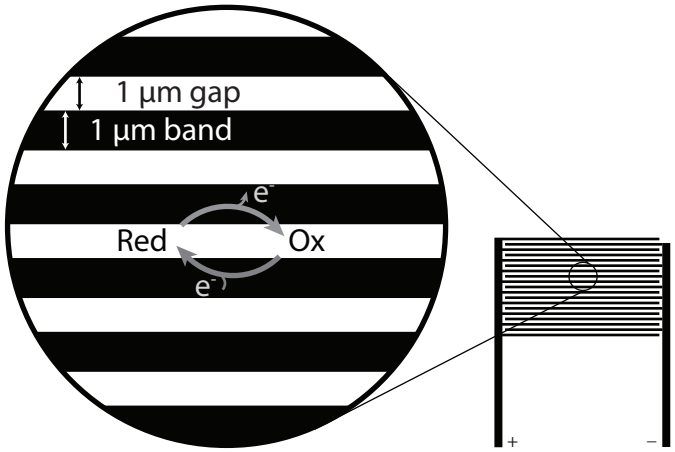

Figure 1.3: Schematic representation of an interdigitated electrode array. One single species can undergo hundreds of reversible redox reactions.

Redox cycling can occur when single molecules repeatedly undergo reduction and reoxidation hundreds or thousands of times between anode(s) and cathode(s) when the electrodes are positioned in very close proximity.

For two planar electrodes, positioned very close to one another, such as in a thin-layer cell, the diffusion of redox species between the two electrodes is practically one-dimensional and the corresponding steady-state current in nano-fluidic channels, where the height of each electrode is much larger than the gap between them, can be described by the following equation

$$I = nFADC/d\,, \tag{1.5}$$

where n is the number of electrons transferred per molecule, F is the Faraday constant, A is the area overlapped between the two electrodes, D is the smaller diffusion coefficient of the two species, C is the bulk concentration of redox species and d is the distance between the electrodes.[17]

This equation assumes that the concentration of supporting electrolyte is much larger than that of the redox species, and also it neglects the fringing of the diffusion profile[2] at the edges of the electrodes (normally, edge effects can be neglected). Current is inversely proportional to the gap width between the electrodes such that the collection efficiency between the anodes and cathodes is almost unity when the gap size is less than 10 μM.[19]

[2]Normally at microelectrodes, mass transport of electroactive species occur from radial diffusion to the edges of the microelectrodes. This phenomenon is called the edge effects and significantly contribute to the overal diffusion of the electroactive species to and from the electrodes. In this case, the rate of mass transfer to and from the electrode and hence the current density, significantly increases as the electrode size decreases.μM.[18]

Simulation studies have recently shown that currents can be significantly enhanced by decreasing the anode-to-cathode gap from 10 μM to 100 nm. However, no further improvements are achieved when the gap width is further reduced. In addition, at such small dimensions, the effect of electrical double layer overlap on the current response becomes an imposition.[20]

Redox cycling can be affected by any kind of surface coating on the electrodes that hinders the transport of redox species to/from the electrodes.[21] Each analyte molecule contributes multiple electrons to the faradaic current, amplifying the detected signal, and may allow single -molecule detection.

Like any other analytical technique, redox cycling possesses limitations. First, it must be applied to species that can undergo reversible redox reactions, and second, like in conventional voltammetry, the employed potential window must be limited to avoid undesirable reactions such as reduction and oxidation of water, dissolved oxygen or solutes.[17]

Wolfrum et al. have shown that amplification factors as high as 104 and detection limits of about 100 molecules can be achieved through the use of nanofluidic thin layer cells having 25-55 nm height.[17]

In conventional amperometry, for a mixture of redox species, e.g. a mixture of two oxidants or two reductants, the detection of the weaker species is obscured by the interference of the stronger one present in the medium, owing to the fact that a more extreme applied potential is required to reduce/oxidize the weaker species, and this will also reduce the other interfering species. Thus, the total steady-state current is affected and consequently, the selectivity is lost. However, this problem can be solved by selectively amplifying the signal from the desired species. For this purpose, different potentials can be applied to anodes and cathodes in an interdigitated electrode array, so that only one species undergoes redox cycling and the other species remains in either oxidized or reduced forms, producing no current at steady-state.[22]

In this thesis, we have introduced cyclic biamperometry as a new method in electroanalytical chemistry. It has been shown that this method, compared to cyclic voltammetry, can be much more sensitive with lower detection limits. Also, this method can be potentially commercialized for application to bioassays and biosensors.

Chapter 2

Experimental

2.1 Materials and Instrumentation

The chemicals used in this study were of highest available quality and were used as received. Potassium chloride (B1098-34) was purchased from EMD™, potassium ferricyanide (13746-66-2), potassium ferrocyanide (60280), 1-naphthol (N-1000) and Buehler micropolish II were bought from Aldrich chemical company Inc, Fluka, Sigma-Aldrich and Tech-Met Canada, respectively.

Ag/AgCl reference electrodes and standard gold electrodes were purchased from Bioanalytical Systems, West Lafayette, IN, USA. The micro-interdigitated gold electrodes (IME1025MAUU and IME0525MAUU) were bought from ABTech Scientific, Richmond, VA, USA. To clean the surface of electrodes from micro-residues a sonicator (Branson-1200 CT, USA) was used and a double-beam UV-Vis spectrophotometer (Cary-100 Varian) was utilized to determine the exact concentrations of reagents in solutions when required. A light microscope, Horiba HR-800, was used to take the micrographs.

All the solutions were made using purified distilled, deionized water from a Barnstead nano-pure water system. All experiments were carried out with a hand-made Faraday cage and the temperature was controlled at $25^\circ \pm 0.1$C with a circulating water bath system from Haake (D1), Germany.

The electrochemical experiments were carried out with a CHI650A potentiostat from CH Instruments, IN, USA. A data acquisition board (NI USB-6251) and LabView™ software were purchased from National Instruments Inc, USA.

2.2 Methods

2.2.1 Electrode Preparation and Determination of Electroactive Surface Area

All the standard gold electrodes used in the experiments were first polished on a piece of soft cloth with Buehler micropolish II (1-micron) and then they were washed with deionized water, put in clean water in the sonicator for 2 minutes and then were gently dried using Kimwipes® tissue paper.

The electroactive surface areas of the electrodes were determined by chronoamperometry using the Cottrell equation

$$i(t) = \frac{nFAD^{1/2}C}{\pi^{1/2}t^{1/2}} = kt^{-1/2}\,, \tag{2.1}$$

where, $i(t)$ is the current in (A), n is the number of electrons, F is the Faraday constant in (C/mol), A is the electroactive surface area in (cm^2), D is the diffusion coefficient in (cm^2/s) of the analyte and C is the concentration of the analyte in (mol/cm^3) in the bulk solution.

Rearranging this equation, we can write

$$i(t) = kt^{-1/2} \qquad \text{or} \qquad i(t) \times t^{1/2} = k \tag{2.2}$$

Therefore, knowing the exact concentration of the analyte, $Fe(CN)_6^{3-}$, and its diffusion coefficient (7.63×10^{-6} cm^2/s) [23] in 0.1 M KCl at 25°C, one can easily calculate the electroactive surface area. To find the exact concentration of ferricyanide using UV-vis spectrophotometry, the extinction coefficient at 419 nm, $\varepsilon = 1.02\times10^3$ $M^{-1}cm^{-1}$ was used.[24]

In our experiments, 5 standard gold electrodes were used which were labeled G1–G5. The electrode surface areas are given in Table 2.1

Label	G1	G2	G3	G4	G5
Surface area $\times10^2$ (cm^2)	2.40	2.39	2.37	2.52	2.43

Table 2.1: Surface area of the standard gold electrodes used in the experiments

2.2.2 Experimental Apparatus

Cyclic Biamperometry

Cyclic biamperometry experiments were carried out with the same potentiostat which was used for cyclic voltammetry. For all CB experiments the working electrode contact from the potentiostat was connected to the G1 electrode and is called

the working-1 (W_1) electrode throughout this thesis. The reference and the auxiliary contacts were both connected to the G2 electrode which is named working-2 (W_2) in this thesis. The ground wire was connected to the Faraday cage in both CB and CV experiments.

For CV experiments G1 was always used as the working electrode. A platinum wire, having a large surface area, and a standard Ag/AgCl reference electrode were used as the auxiliary and the reference electrodes, respectively.

In CB experiments the voltage window was -0.4 V — +0.4 V and that for CV was -0.2 V — +0.6 V unless otherwise stated.

Monitoring the Potential Profile

To monitor the potential profile at the solution-electrode interface of the W_1 electrode in CB experiments a data acquisition board with two input channels was used. Channel I was connected to an Ag/AgCl reference and the G1 electrode. Channel II, which served as the control channel, was connected to the G1 and G2 electrodes to monitor the applied voltage profile by the potentiostat. A program was written in LabView^{TM} software to read the input voltage values from both channels every 0.01 s. (Figure 2.1)

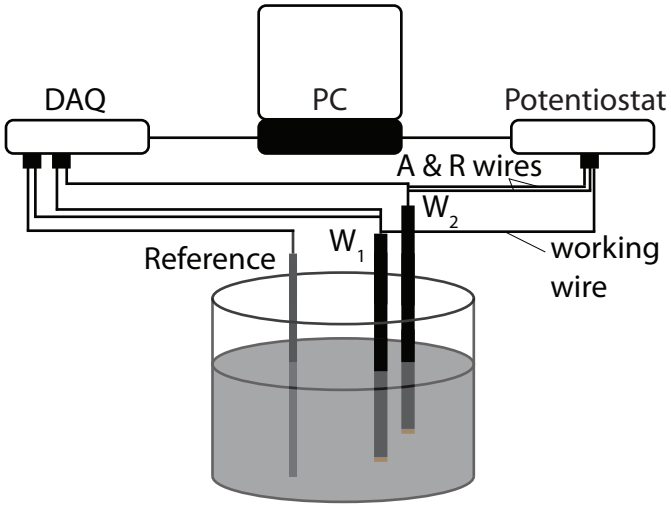

Figure 2.1: Apparatus for monitoring potential profile at the W_1 electrode. The DAQ board is connected to the Ag/AgCl reference electrode and the G1 electrode through channel I and the channel II (control) was connected to the G1 and G2 electrodes. The potentiostat is connected to G1 through the working contact and both auxiliary and reference contacts are connected to G2.

Interdigitated Electrodes

The physical surface areas of the IDEs were calculated based on the band and gap sizes provided by the manufacturer. The non-interdigitated parts of the electrode had been covered with a non-conductive dye which made it easy to calculate the surface area. For this study only two different sizes were used and these were connected to the potentiostat through a commercially available adapter. (Figure 2.2). The related information about the IDEs is provided by the manufacturer in Table 2.2.

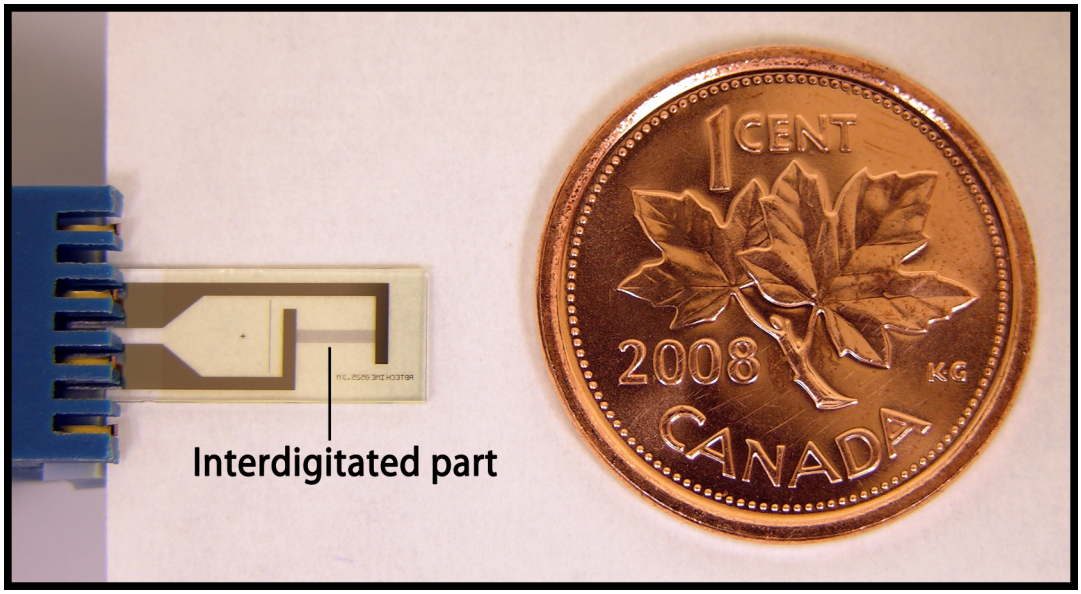

Figure 2.2: IME0525.3MAUU Interdigitated electrodes

	IME1025.3MAUU	IME0525.3MAUU
Digit length, d (μm)	2990	2995
Number of digit pairs, N	25	25
Digit width, a (μm)	10	5
Interdigit space, a (μm)	10	5
Surface area of W_1, A (cm^2)	$7.4_{75} \times 10^{-3}$	$3.7_{44} \times 10^{-3}$

Table 2.2: The dimensions of the gold IDEs used in the experiments. These values were provided by the manufacturer and the surface areas of W_1 electrodes were manually calculated based of the information obtained from the manufacturer.

Stoichiometry of the reaction of 1-Naphthol with ferricyanide

To represent a practical application of cyclic biamperometry, the stoichiometry of the reaction between 1-naphthol and ferricyanide was investigated. 1-Naphthol is

known to react with ferricyanide to produce ferrocyanide and an oligomer which precipitates in the aqueous phase.

For this purpose, the concentration of ferricyanide was kept constant at 3.00 mM in a 2.00 mL beaker and 1-naphthol was added into the solution. After the addition of each aliquot, CB was applied to the solution and the i_p values were recorded. Thus, a titration curve was produced.

Chapter 3

Results and Discussion

The peak currents in cyclic voltammetry are described by the Randles-Sevcik equation (Eq. 3.1). Thus, any variation in the ratio of reduced:oxidized concentrations will not result in any change in peak currents, provided that the total concentration is constant.

$$i_p = (2.69 \times 10^5) n^{3/2} A D^{1/2} C \nu^{1/2} \,, \tag{3.1}$$

In cyclic biamperometry, however, peak currents are limited by one of the two halves of a redox couple. For example, if the two working electrodes have identical areas, and if the diffusion coefficients of the two redox forms are the same, then the species present at the lower concentration will limit the measured peak current. However, since this form is generated in equal concentration on the reverse sweep, peak currents in biamperometry are expected to be twice those predicted by the Randles-Sevcik equation if the area of only one of the electrodes and the concentration of the limiting species are considered. More complicated situations exist when electrodes have significantly different areas and when the concentration ratio for the two redox forms is close to 1:1.

Figures 3.1 and 3.2 show voltammograms and biamperograms, respectively, for a 1.00 mM ferricyanide solution, using the same electrode (W_1) for both techniques, and using an electrode of approximately equal area for W_2 in the biamperometric scans. The solution for biamperometry also contained 5.0 mM ferrocyanide. The applied scan rates were 10, 25, 50, 75, 100, 125 and 150 mV/s. Figure 3.3 shows plots of cathodic peak current, i_{pc}, against the square root of the applied scan rate for both techniques.

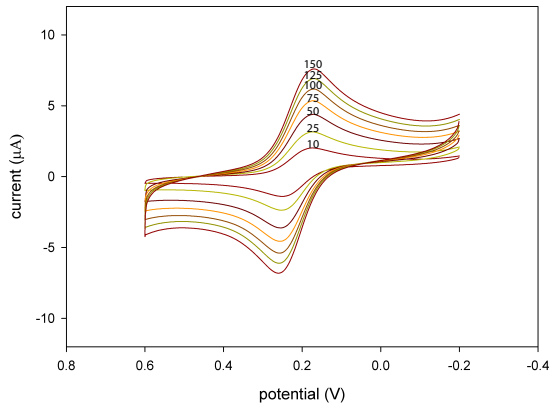

Figure 3.1: Voltammograms for a 1.00 mM ferricyanide solution at different scan rates. The scan rates have been shown on the curves.

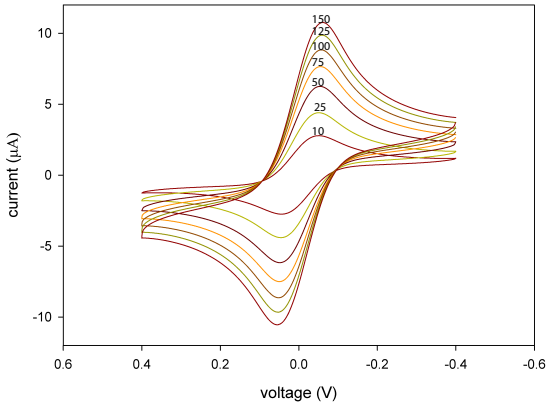

Figure 3.2: Biamperograms for a solution of 1.00 mM ferricyanide and 5.00 mM ferrocyanide, using the same working electrode as W_1 and a similar electrode as W_2. The scan rates have been shown on the curves.

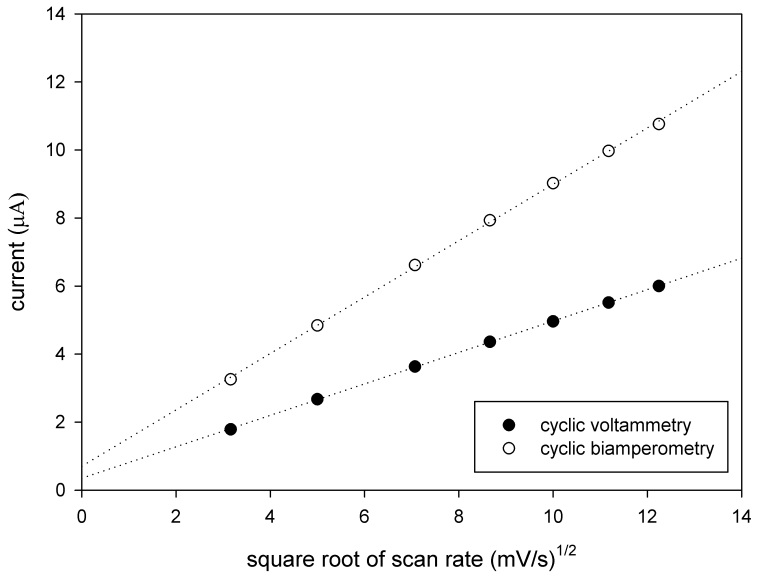

Figure 3.3: Plots of cathodic peak current, i_{pc}, against the square root of the applied scan rate for both techniques. The slopes of the linear trend lines are 0.828 and 0.462 for CB and CV, respectively. The y-intercept and R^2 values for CB and CV are 0.701, $R^2 = 0.999_6$ and 0.351, $R^2 = 0.999_9$, respectively.

Under these conditions, with approximately equal area W_1 and W_2 electrodes, the maximum peak currents for CB are obtained when the concentrations of the two redox forms are nearly the same in a series of solutions containing a constant total concentration of $Fe(CN)_6^{3-}/Fe(CN)_6^{4-}$ (Figure 3.4). In addition, CB peak

currents are nearly the same as those found with CV when the concentrations of the two redox forms are equal (Figure 3.5).

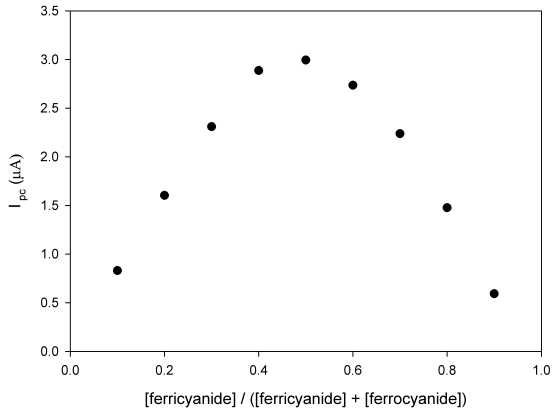

Figure 3.4: When the electrode surface areas are nearly the same, the maximum peak currents in CB are obtained when concentrations of ferri/ferrocyanide are equal. Scan rate is 50mV/s.

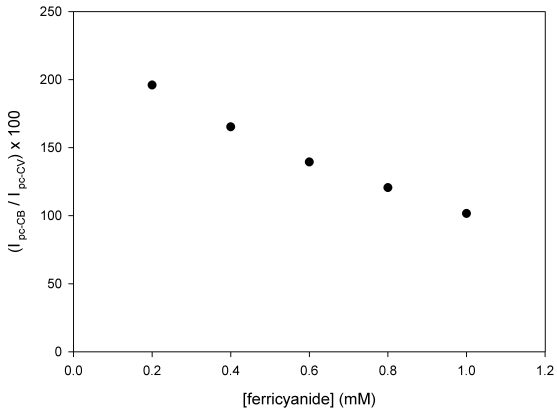

Figure 3.5: CB peak currents are nearly the same as those found with CV when the concentrations of the two redox forms are equal. Scan rate is 50 mV/s.

CV allows precise control of the potential difference across one working electrode-to-solution interface, through the use of a reference electrode. With CB, on the other hand, only the applied voltage is controlled, while the distribution of potential differences across the two interfaces is determined by the species present in the solution and at which electrode the limiting process occurs. To demonstrate this, the voltage distribution across the two electrodes and the potential profile at the W_1 electrode-solution interface were monitored using a National Instruments Model NI USB 6251 data acquisition board with LabView^{TM} software.

On the data acquisition board two channels were used. Channel l was connected to W_1 and an Ag/AgCl reference electrode. Channel 2 was connected to the W_1 and W_2 electrode leads as a control channel to monitor the applied triangular voltage waveform while at the same time cyclic biamperometry was applied to a series of solutions containing a constant total $Fe(CN)_6^{3-} + Fe(CN)_6^{4-}$ of 1.00 mM (Figure 2.1).

Figure 3.6 represents the plot of measured potential at W_1 versus applied voltage across the two electrodes at a fixed scan rate of 50 mV/s and the ratios of the redox species for the curves shown in this figure are given below (Table reftable:VoltageDistribution).

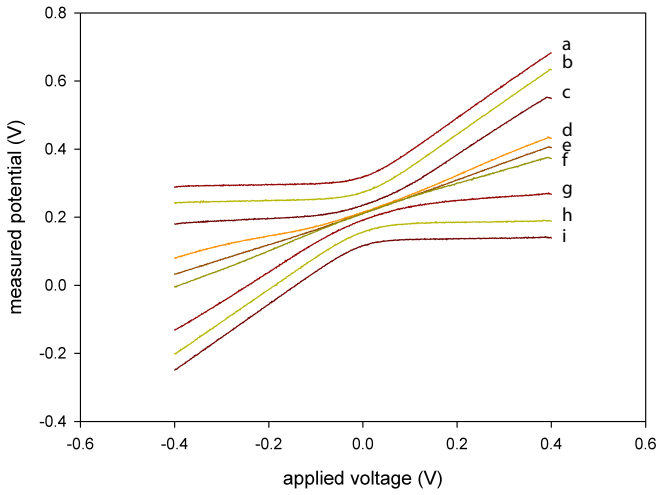

Figure 3.6: Measured potential versus applied voltage at electrode-solution interface in CB. When one of the species is in excess the voltage distribution across the two electrodes is not symmetrical, and also the reaction of the limiting species occurs at the electrode that has the greater interfacial potential difference. In other words, the applied voltage distributes in such a way that maximum current is achieved.

Label	a	b	c	d	e	f	g	h	i
Ratio	50/1	10/1	2/1	1.1/1	1/1	1/1.1	1/2	1/10	1/50
Maximum potential scan rate (mV/s)	48.2	47.9	44.3	33.8	28.3	26.9	45.4	49.5	49.4

Table 3.1: The ratios $[Fe(CN)_6^{-3}]/[Fe(CN)_6^{-4}]$ for the curves shown in figure 3.6 and the measured maximum W_1 potential scan rates, from an applied voltage scan rate of 50 mV/s

Based on the observation of this experiment, an equivalent circuit is proposed to help us to understand the behavior of the system.

In the electrochemical cell of our study this behavior of cyclic biamperometry can be approximated with the equivalent circuit shown in figure 3.7. There are two working electrode-solution interfaces which are separated by a solution resistance, and each interface is characterized by a double-layer capacitance in parallel with an electrochemical impedance.

This equivalent circuit is proposed by manipulating the present equivalent cicuit for cyclic voltammetry in which only W_1, Z_1, C_{dl-1} and R_Ω are shown because in cyclic voltammetry only the reaction occuring at W_1 is of interest and the opposite reaction taking place at the auxiliary electrode does not affect the overal current.

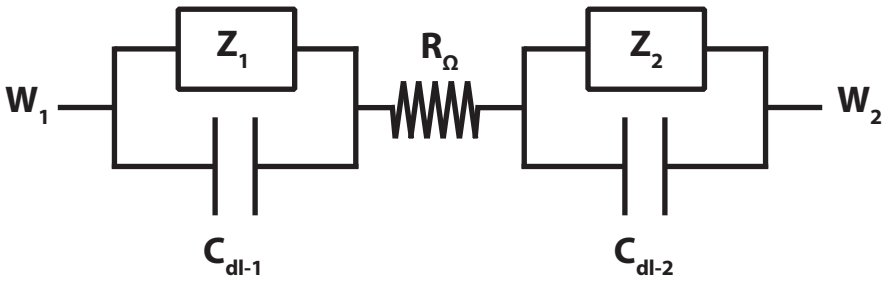

Figure 3.7: An equivalent circuit for the electrochemical cell in this study. R_Ω is the solution resistance, Z_1 and Z_2 are general impedances and $C_{dl\text{-}1}$ and $C_{dl\text{-}2}$ are the double layer capacitances at the W_1 and W_2 electrode-solution interfaces, respectively.

Based on this equivalent circuit, one can reason that if the concentration of both redox species and the corresponding diffusion coefficients are the same and also if the electroactive surface areas of the electrodes are equal to each other, the total impedance values at each electrode-solution interface must be equal to one another. But, if, one of the species is in great excess, for example, ferricyanide, and reaction of that speices occurs at the W_1 electrode, for example, reduction of ferricyanide at the W_1 electrode, logically, the impedance at W_1 electrode-solution interface must decrease or in other words, more of the applied voltage is sensed across W_2-solution interface.

It then follows that the distribution of interfacial potential differences in cyclic biamperometry should be asymmetrical when the electrode surface areas and/or the diffusion coefficients of the redox species are not equal.

Based on these findings, it is obvious that variations at the electrode surface areas can directly affect the peak currents through changing the impedance values at the electrode-solution interfaces.

Thus, in cyclic biamperometry, unlike cyclic voltammetry, another factor also affecting the peak current is the electroactive surface area of the W_2 electrode. Figure 3.8 represents the dependence of cathodic CB peak current on the surface area of the W_2 electrode, which was varied by the electrical connection of additional electrodes of approximately equal area to W_2. In this experiment, ferricyanide was present at 7 times the concentration of ferrocyanide in the solution. The curve asymmetry is believed to be due to the increased capacitance as a result of the increased area at the W_2 electrode-solution interface, since the limiting reaction (oxidation of ferrocyanide) occurs at the multi-electrode W_2.

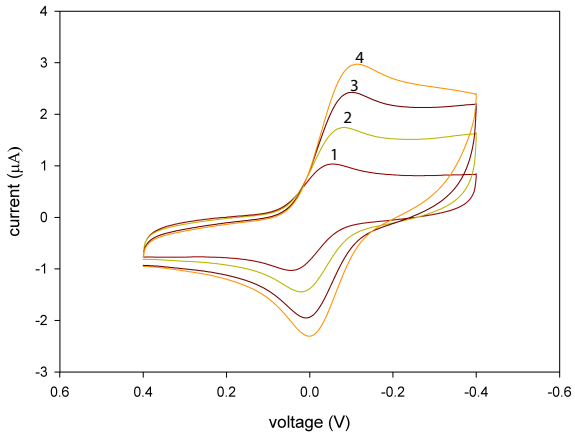

Figure 3.8: Biamperograms for a solution containing a total ferri/ferrocyanide concentration of 2.00 mM at the ratio of 7:1; The effect of adding more electrodes to W_2. Scan rate = 25 mV/s. The total number of electrodes connected to W_2 is shown on the plots.

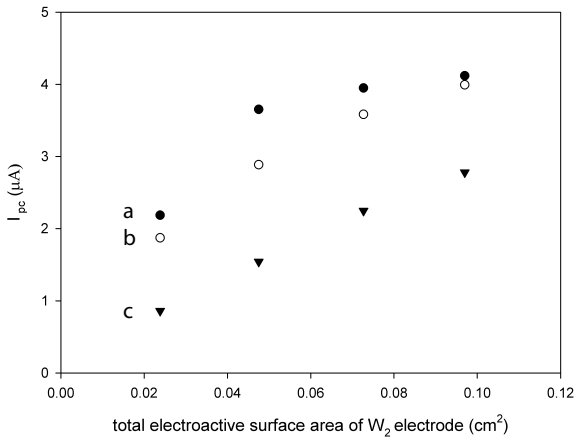

Figure 3.9: Dependence of cathodic CB peak current on the surface area of the W_2 electrode at different ratios of $[Fe(CN)_6^{-3}]$: $[Fe(CN)_6^{-4}]$. (a) 1:1 (b) 3:1 (c) 7:1. $[Fe(CN)_6^{-3}] + [Fe(CN)_6^{-4}] =$ 2.00 mM and scan rate is 25 mV/s.

Figure 3.9 shows results of the same CB experiment, in which the cathodic peak currents are plotted as a function of W_2 electroactive surface area, for different ratios of $Fe(CN)_6^{3-} + Fe(CN)_6^{4-}$. When one of the redox forms is present in great excess, the peak current is linearly proportional to the electroactive surface area of the W_2 electrode.

These results show that in cyclic biamperometry, peak current is limited by the product $AD^{1/2}C$, and these values can be determined for each species at each electrode. Generally, with equal area W_1 and W_2 electrodes, one of the two halves of the redox couple will limit the magnitude of the peak currents observed. However, under conditions of asymmetric electrode areas and close to equivalent concentrations, the W_1 process (for larger W_2) can limit current magnitudes for both forward and reverse CB scans.

For analytical purposes, a linear response, a good detection limit and high sensitivity are desired. Therefore, keeping the concentration of one of the species in excess and providing a large W_2 electrode, the signal, due to the production of the limiting species during the course of a reaction, can be amplified.

3.1 Applications of Cyclic Biamperometry

3.1.1 Stoichiometry of the Reaction between Ferricyanide and 1-Naphthol

In this study, the stoichiometry of the reaction between ferricyanide and 1-naphthol was determined using cyclic biamperometry. This reaction was chosen not only because 1-naphthol is able to instantaneously react with ferricyanide to produce ferrocyanide but also it is one of the products in the dephosphorylation of 1-naphthyl phosphate by alkaline phosphatase and this is one of the most widely used enzymes in bioassays.

Figure 3.10 shows the result of a cyclic biamperometric dead-stop titration of ferricyanide with 1-naphthol. In this experiment, the exact concentration of ferricyanide and 1-naphthol solutions were spectrophotometrically determined using $\varepsilon_{419} = 1.02 \times 10^3$ cm^{-1}M^{-1}[24] and $\varepsilon_{213} = 4.48 \times 10^4$ cm^{-1}M^{-1}[25], respectively.

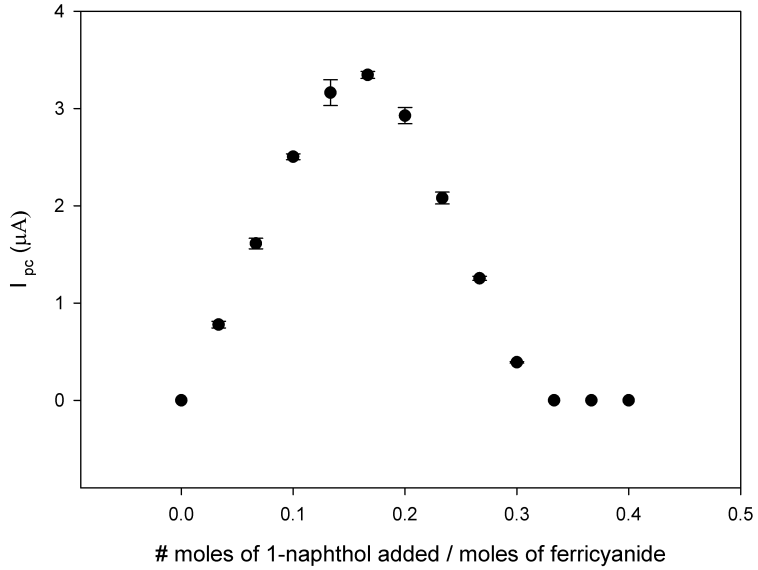

Figure 3.10: In the reaction between 1-naphthol and ferricyanide, 3 ferricyanide ions are reduced per 1-naphthol molecule. $[Fe(CN)_6^{3-}] = 3.0mM$, [1-naphthol] = 1.0 mM; Scan rate = 25 mV/s and $A_{W_1} = 2.40 \times 10^{-2}$ and $A_{W_2} = 2.39 \times 10^{-2}$ cm^2

During the experiment, the initial concentration of ferricyanide present in these solutions was maintained constant, and increments of 1-naphthol were added. The graph intersects the x-axis at a 1-naphthol:ferricyanide ratio of 0.33, indicating that 3 ferricyanide ions are reduced per 1-naphthol molecule. A dimerization of naphthoxy radicals followed by two 2-electron oxidations can explain this stoichiometry.[26] This product is called Pummerer's ketone analog.[27]

The following schemes illustrate the possible pathways of oligomerization of 1-naphthol and electron transfer to ferricyanide. Scheme 3 is the only one of these that explains the 3:1 ferricyanide:1-naphthol stoichiometry.

Oxidation of 1-naphthol by one equivalent of ferricyanide results in an unstable naphthoxy radical. Resonance structures show that the unpaired electron can be present either at position 2 or position 4 of the naphthoxy structure (Schemes 1 and 3, top) or on the second ring (Scheme 4, structures 5 and 7). Possible dimerization of a naphthoxy radical with the single electron at position 2 and a naphthoxy radical with the single electron at position 4 (Scheme 1) results in formation of an aromatic ketone that, following an internal cyclization, can be further oxidized in a 2-electron process. Further $1e$ oxidation of this product, coupling with naphthoxy radical, cyclization and 2e oxidation yields an overall stoichiometry of 4 electrons per residue added to the polymer. Based on results of the stoichiometry experiment, this pathway is unlikely or not dominant.

Other polymerization pathways are possible, such as the one shown in Scheme 2. In this example, the dimer, initially formed by the combination of two naphthoxy radical with unpaired electrons at position 2, can be oxidized ($1e$) to a radical that can react with an additional naphthoxy radical. The ultimate product(s), when fully oxidized, yield a stoichiometry of 4 electrons per residue added. Again, this pathway is unlikely or not dominant.

In Scheme 3, two dimerization pathways are shown in which polymer formation would not occur. The pathway on the left shows dimerization of two naphthoxy radicals with the unpaired electrons on position 4. If this pathway proceeds the end product would be a stable dimer and two electrons would be transferred per molecule of 1-napthol. However, if the pathway on the right proceeds, dimerization and formation of the final stable product would result in transfer of three electrons per molecule of 1-napthol. The cyclization process has been documented for substituted phenols, which form compounds called Pummerer's ketone analogs. The initial cyclised product can undergo a $4e$ oxidation to form the final structure (bottom right of Scheme 3) which would be expected to be insoluble in aqueous buffers. To date, this is the only process that can account for the overall 3:1 ferricyanide:naphthol stoichiometry determined using CB measurements in this work. Scheme 4 presents an overall summary of possible reactions along with their predicted stoichiometries, and suggests that if 2-methyl-1-naphthol were used instead of 1-naphthol, the proposed n=3 reaction would not occur. Further experimentation could thus confirm this pathway, but is beyond the scope of this thesis.

Scheme 1

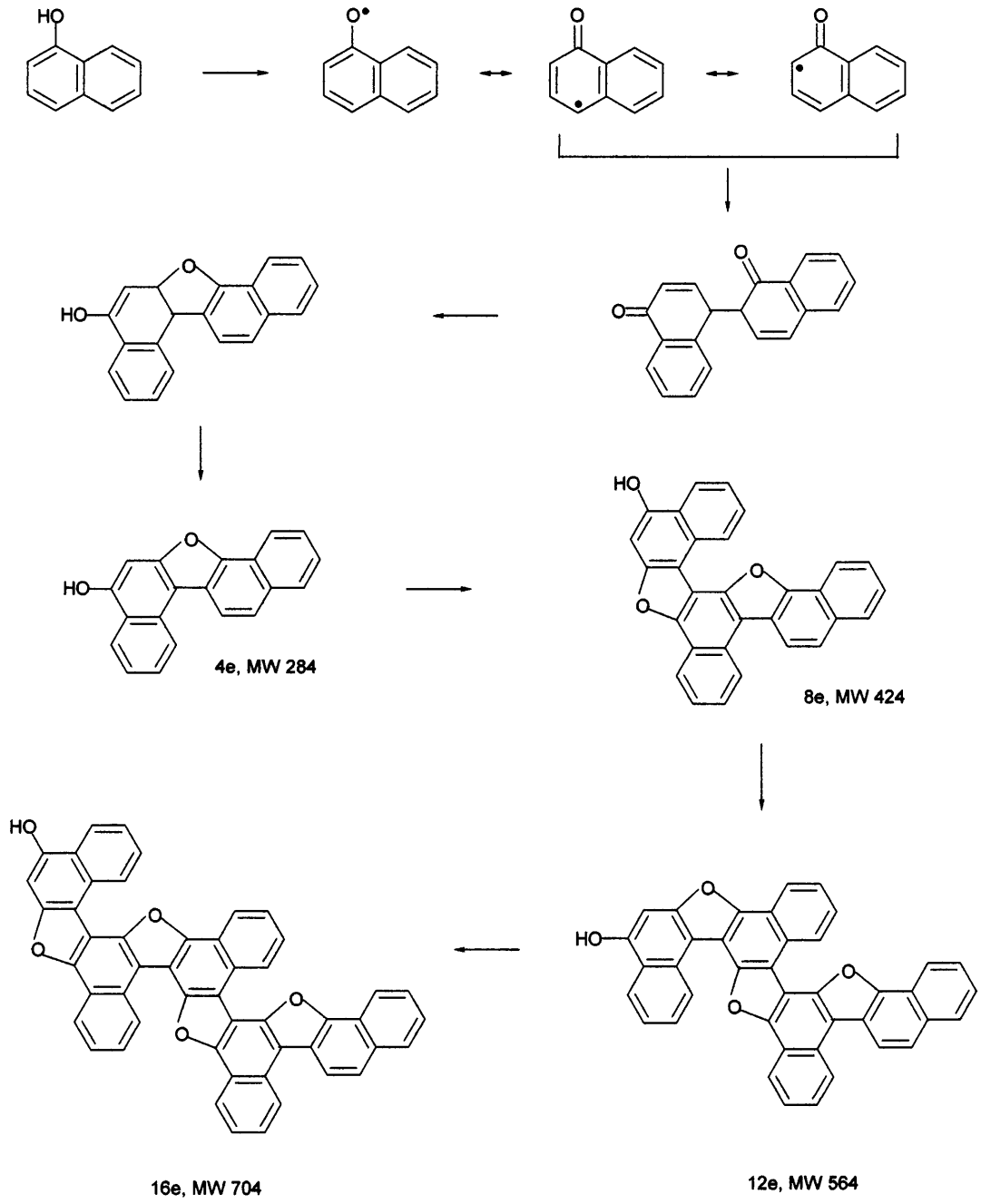
HO
O•
O
O
HO
O
O
O
HO
O
4e, MW 284
HO
O
O
8e, MW 424
HO
O
O
O
O
16e, MW 704
HO
O
O
O
12e, MW 564

Scheme 2

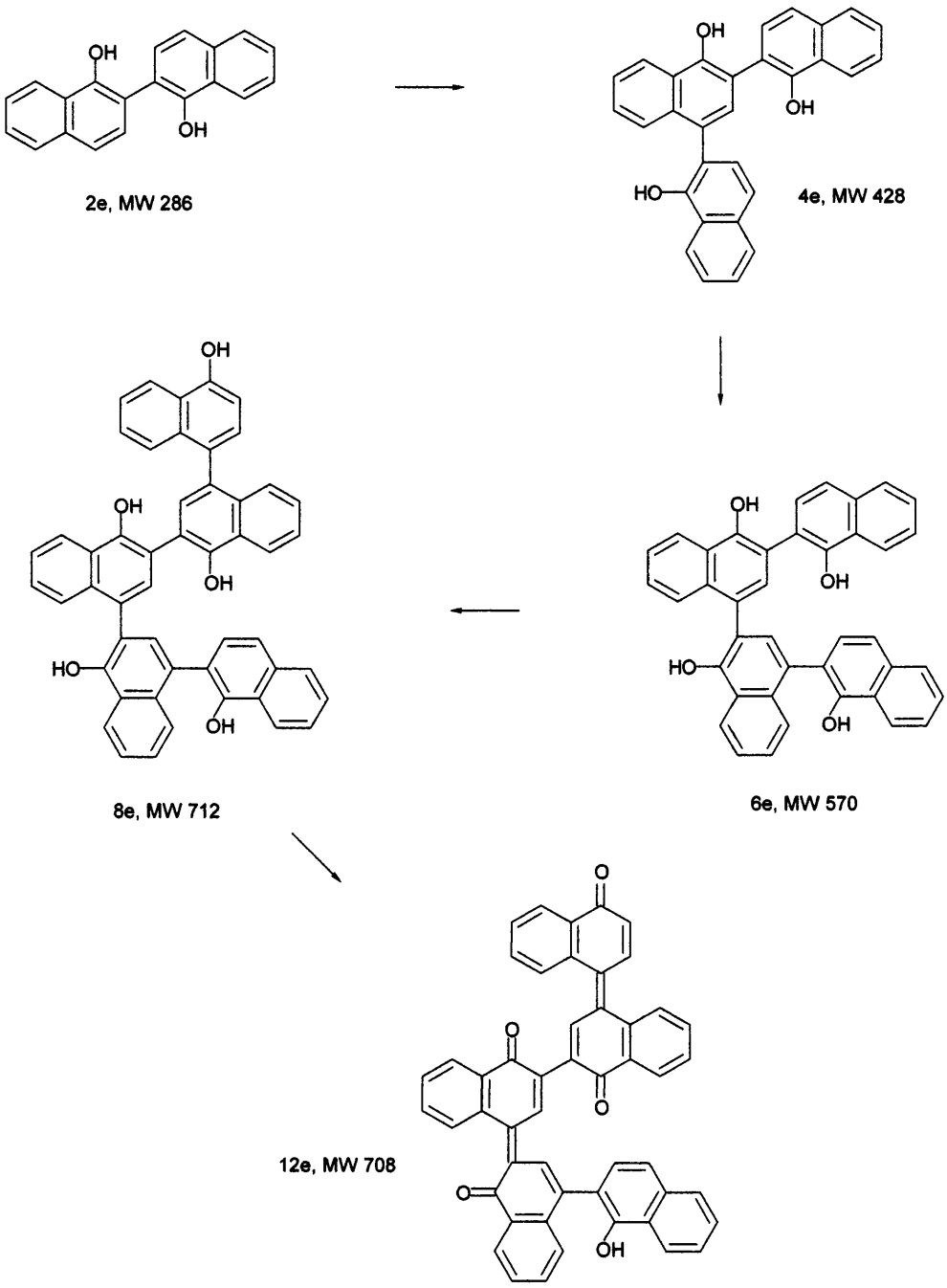
OH
OH
2e, MW 286
OH
OH
HO
4e, MW 428
OH
OH
HO
6e, MW 570
OH
OH
OH
HO
OH
8e, MW 712
O
O
O
O
OH
12e, MW 708

Scheme 3

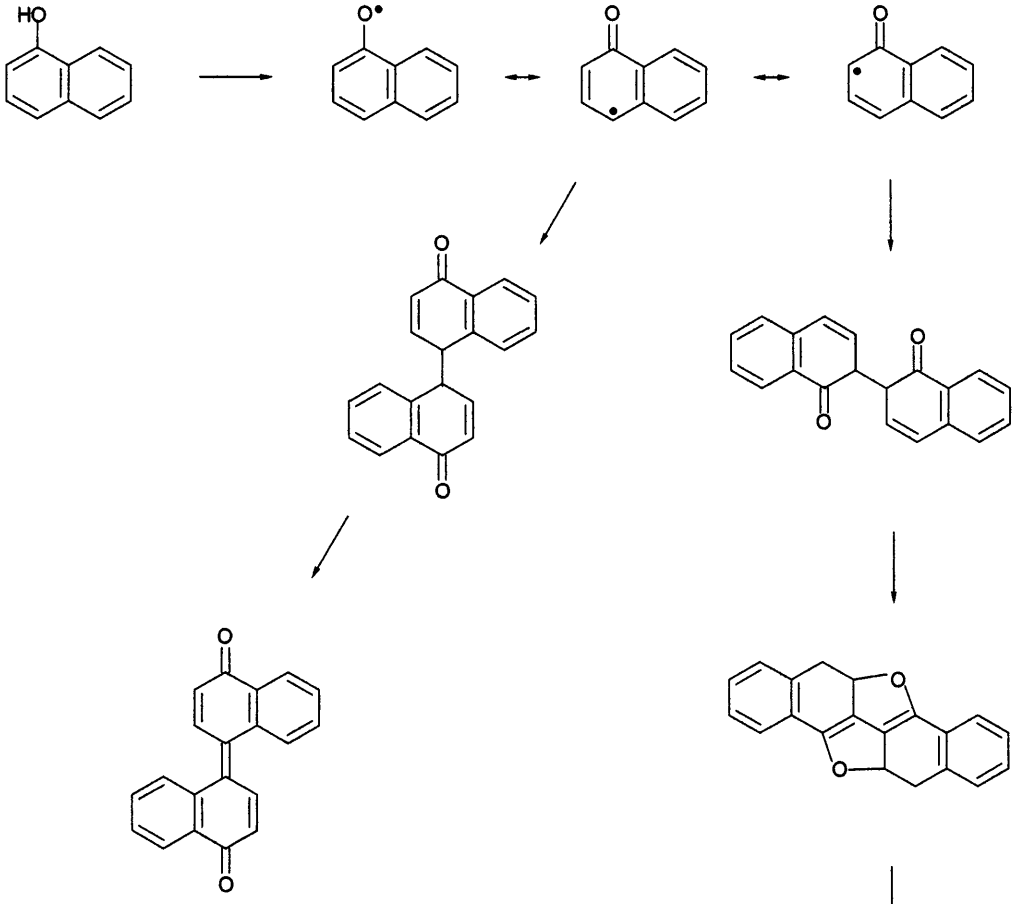

Scheme 4

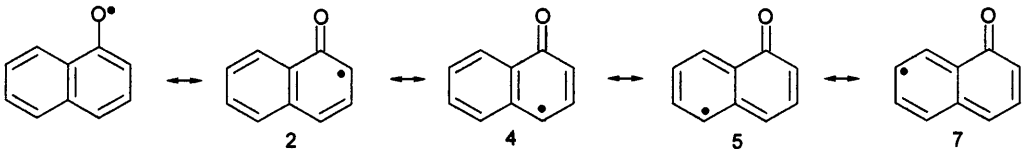

Numbers indicate position of radical on naphthyl skeleton

n = moles ferricyanide consumed per mole naphthol

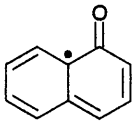

This is the most stable radical, but it is unreactive.
If a dimer forms, it cannot be oxidized, so n=1.

2+2 : dimer, n = 3, reaction stops
2+4 : polymer, n = 4 per residue added
2+5 : polymer, n = 4 per residue added
2+7 : polymer, n = 4 per residue added
4+4 : dimer, n = 2, reaction stops
4+5 : dimer, n = 2, reaction stops
4+7 : dimer, n = 2, reaction stops
5+5 : dimer, n = 2, reaction stops
5+7 : dimer, n = 2, reaction stops
7+7 : dimer, n = 2, reaction stops

Ferricyanide provides an oxidizing environment, thus any hydroquinones formed by radical combination are assumed oxidized immediately.

If the 2-position were blocked by a methyl group (2-methyl-1-naphthol) the n=3 reaction would not occur.

3.1.2 Cyclic Biamperometry with Interdigitated Electrodes

Interdigitated electrodes (IDEs) consist of a set of closely and alternately positioned anodes and cathodes. IDEs of two different sizes, the dimension of which are given in Table 2.2, were used in this work.

The surfaces of the gold segments connected to the interdigitated part of the electrodes were covered with an insulator dye by the manufacturer so that redox reactions only occur on the interdigitated part of the electrodes and not on the connecting leads. Also the geometric surface areas can be easily calculated based on the physical dimensions.

Figure 3.11 shows a micrograph (taken by a HR-800 Horiba light microscope) of the IME0525.3MAUU interdigitated electrodes illustrating the insulator dye.

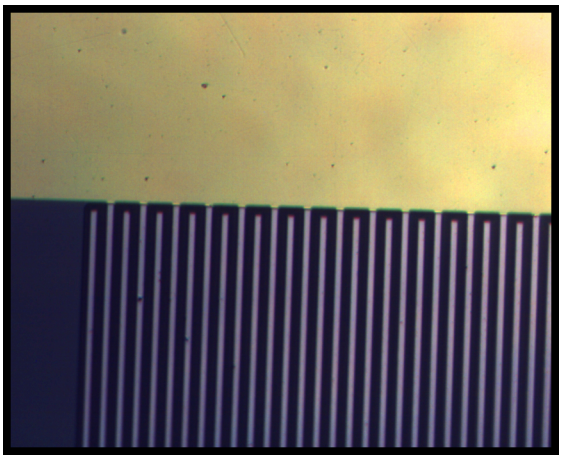

Figure 3.11: A micrograph of the IME0525.3MAUU interdigitated electrodes

Two sets of experiments were carried out with the IDEs. In the first set, the limiting currents in CB and peak currents in CV were compared based on variations of scan rate. Figures 3.12 and 3.13 show the shape of the CB and CV curves at 4 mV/s, respectively. Due to the redox cycling effect, no depletion occurs at the electrode-solution interface with IDEs and consequently no peak is observed. Sigmoid-shaped plots are characteristic of redox cycling at micro-interdigitated electrodes.[20]. Instead of peak current, the limiting current is measured by extending the baseline and measuring the vertical line segment between the graph and the extended baseline (Figure 3.12).

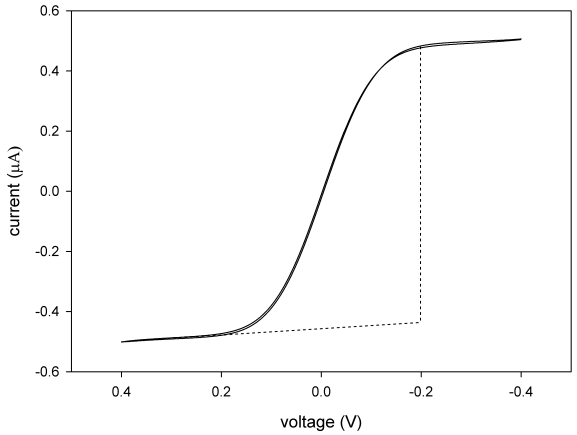

Figure 3.12: CB for a solution containing 0.20 mM ferricyanide and 0.20 mM ferrocyanide at the smaller IDEs. Scan rate is 2 mV/s

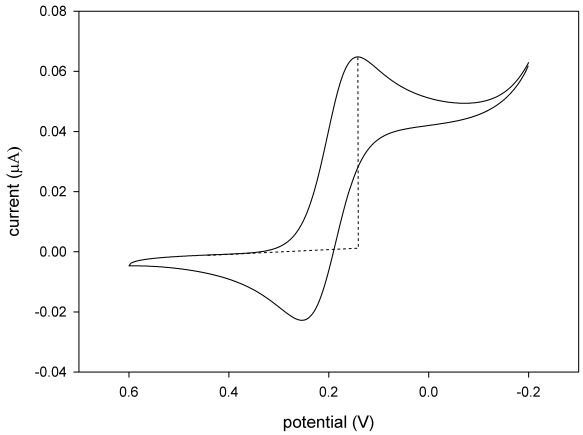

Figure 3.13: CV for a solution containing 0.20 mM ferricyanide at the smaller IDEs. Scan rate is 2 mV/s

Figures 3.14 and 3.15 show the dependence ofthe limiting and the peak current on scan rate using IDEs in CB and CV. In experiments with IDEs, the same electrode used as W_1 in CB was connected to the working wire in CV to make sure that the electroactive surface area of W_1 for both techniques remains unchanged. Surprisingly, as shown in the graphs, limiting currents in cyclic biamperometry are independent of scan rate. This is very beneficial because, keeping the scan rate very low, the experimenter can minimize the charging current and the subsequent noise level, resulting in very high signal to noise ratio at low concentrations.

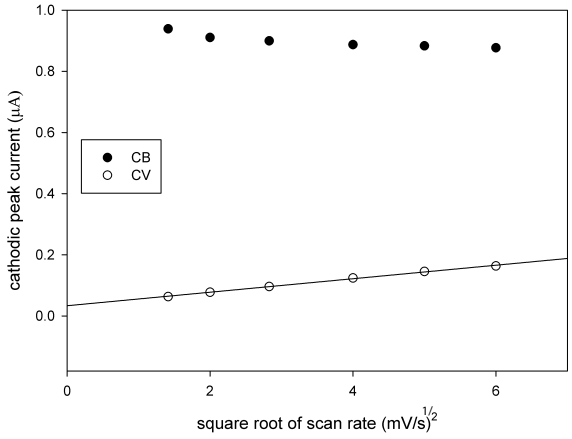

Figure 3.14: Comparison of the limiting and the cathodic peak currents at the smaller IDEs for CB and CV. For CB, [ferricyanide] = [ferrocyanide] = 0.20 mM and for CV, [ferricyanide] = 0.20 mM. The slope of the linear regression line and the y-intercept for CV is 0.0221 and 0.0336, respectively. R^2 value is 0.9979.

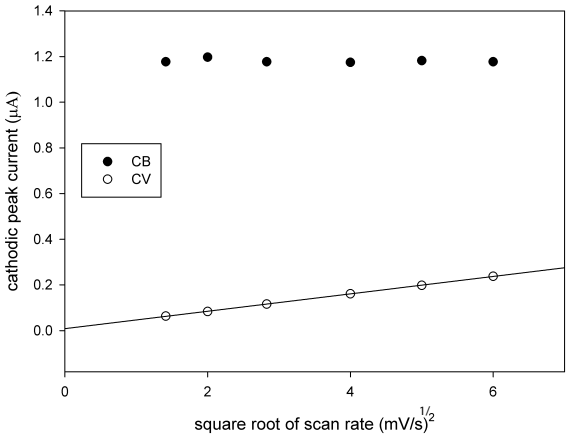

Figure 3.15: Comparison of the limiting and the cathodic peak currents at the larger IDEs for CB and CV. For CB, [ferricyanide] = [ferrocyanide] = 0.20 mM and for CV, [ferricyanide] = 0.20 mM. The slope of the linear regression line and the y-intercept for CV is 0.0381 and 0.0088, respectively. R^2 value is 0.9999.

Figures 3.16 and 3.17 show plots of the ratio of limiting CB current to CV peak current as a function of square root of scan rate, for the 5 μm and 10 μm IDEs, respectively. These plots clearly show that at lower scan rates, the CB signal amplification due to redox cycling, is very large with values of 14.8 and 18.5 reached at the lowest scan rate investigated (2 mV/s) for the smaller and the larger IDEs, respectively.

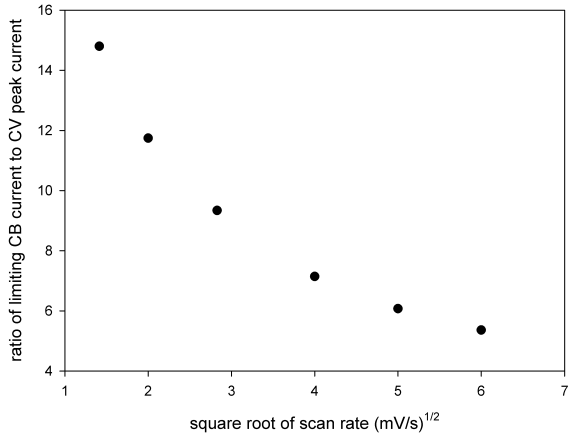

Figure 3.16: Ratio of limiting CB current to CV peak current for the smaller IDEs. The numbers were obtained from dividing the CB limiting current values by the CV peak current values in Figure 3.14

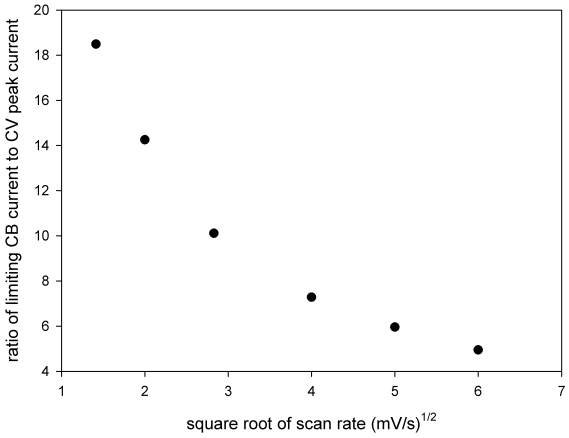

Figure 3.17: Ratio of limiting CB current to CV peak current for the larger IDEs. The numbers were obtained from dividing the CB limiting current values by the CV peak current values in Figure 3.15

Figure 3.18 shows the variation of current with concentration at 25 mV/s with the smaller IDEs.

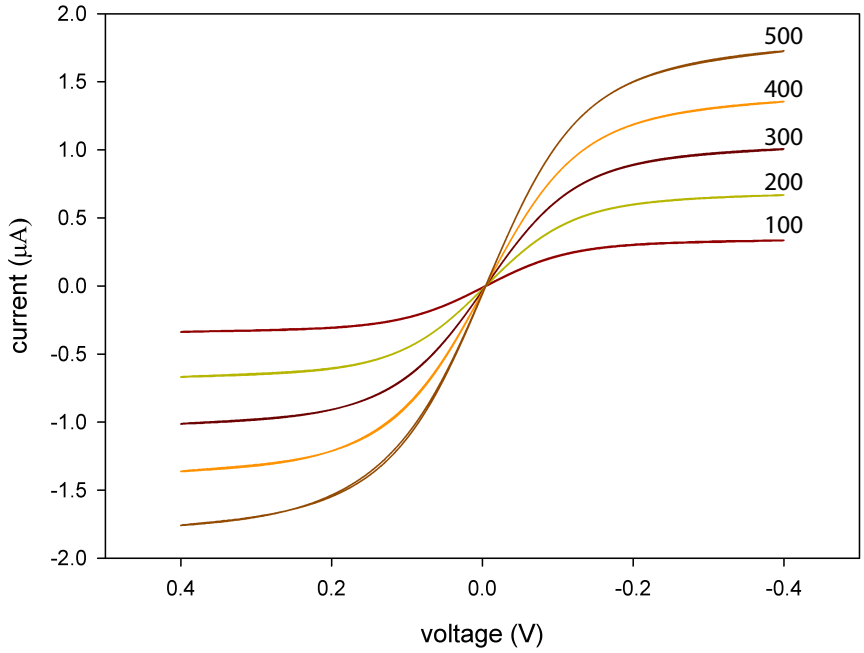

Figure 3.18: Plot of current versus applied voltage for varying concentration of ferricyanide and ferrocyanide at the smaller-dimension IDE. Due to redox cycling, the common depletion effect at the electrode surface does not occur and consequently the graphs have a sigmoid-shape with no peaks. In each case ferricyanide and ferrocyanide were equimolar and the concentrations were increased from 100 to 500 μM. The equimolar concentrations of ferri and ferrocyanide have been shown on each plot.

Figures 3.19 and 3.20 represent the cathodic peak current in CV and the limiting current obtained at 200 mV in CB against concentration using the interdigitated electrodes. In the CB experiments, ferrocyanide concentration (zero in the CV experiments) was kept the same as that of ferricyanide in each solution.

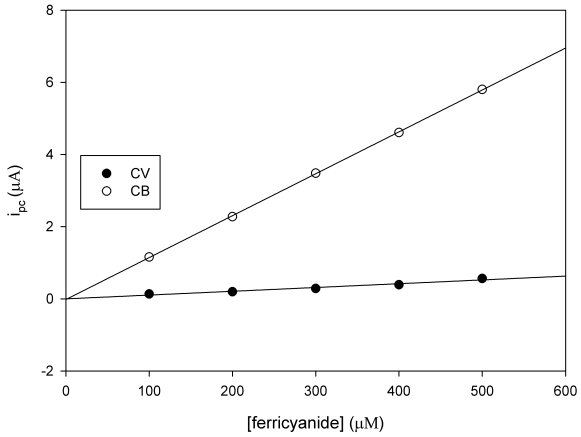

Figure 3.19: Comparison of the cathodic peak currents at the smaller IDEs for CV and the limiting current at 200 mV for CB. The slopes of the linear regression line for CB and CV are 0.0116 and 0.0010 and the y-intercepts for CB and CV are -0.0177 and -0.0002 and the R^2 values for CB and CV are 0.9999 and 0.9796, respectively.

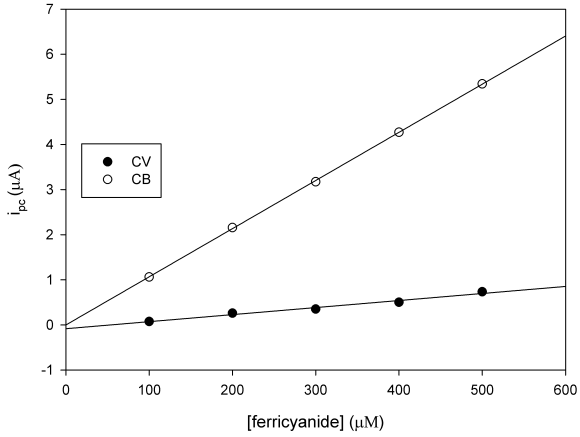

Figure 3.20: Comparison of the cathodic peak currents at the larger IDEs for CV and the limiting current at 200 mV for CB. The slopes of the linear regression line for CB and CV are 0.0107 and 0.0016 and the y-intercepts for CB and CV are 0.0008 and -0.0836 and the R^2 values for CB and CV are 0.9999 and 0.9644, respectively.

As shown in these figures, CB at interdigitated electrodes is a much more sensitive technique, compared to CV. Although sensitivity and detection limit do not represent the same concept, usually improved sensitivity leads to a lower detection limit. To find the detection limit of CB at interdigitated electrodes, a series of dilute solutions, 4-18 μM ferricyanide containing an equimolar amount of ferrocyanide, was prepared and subjected to cyclic biamperometry at 10 mV/s using the smaller IDEs. The detection limit, based on standard deviation of $y-$intercept ($3s_b/m$), was determined to be 2.6×10^{-7} M and this is much lower than the detection limit obtained by a corresponding CV method, 19 μM. The detection limit for CV was determined using a standard-size gold electrode ($A = 2.40 \times 10^{-2}$) cm^2 that has a much larger geometric surface area than the 5 μm IDE ($A = 3.7_{44} \times 10^{-3}$), and consequently should result in more sensitive measurements.

Taken together, these results show that CB at IDEs allow approximately 2 orders of magnitude improvement in detection limits in comparison with standard CV methods. This improvement is expected to lead to much precision and accuracy in bioassays (where electrochemical methods are used), such as in the family of enzymatic or immunoassays where alkaline phosphatase is used as an indicator enzyme or as an antibody label. The substrate, 1-naphthyl phosphate , is dephosphorylated by the enzyme, resulting in production of 1-naphthol, which instantaneously reduces ferricyanide and generates ferrocyanide, allowing sensitive CB measurements.

Chapter 4

Summary and Suggestions for Further Research

In this thesis, cyclic biamperometry as a new method in electroanalytical chemistry was introduced. Due to similarities between this method and cyclic voltammetry, it was compared to CV and both advantages and disadvantages were discussed.

The most obvious advantage of cyclic biamperometry over cyclic voltammetry is the simplicity of the apparatus and lack of a reference electrode in the system.

It was shown that CB can exhibit a much more sensitive response, compared to CV, through (i) adjusting the concentration of the redox species in the solution so that presence of one redox-active analyte in great excess amplifies the sensitivity up to two fold for electrodes of equal area, (ii) increasing the surface area of the W_2 electrode which proportionally increases the sensitivity provided that one of the species is present at least in the same proportional excess amount in the solution; for example, by 5 times increasing the area of W_2, the peak currents will increase 5 times provided that one species is present at least 5-fold excess over the other and (iii) use of micro-interdigitated electrodes that results in at least 10 times amplification (depending on the size/gap of the electrodes) of the sensitivity through the redox cycling effect.

Perhaps the disadvantages of cyclic biamperometry are (i) lack of control over potential of individual electrodes so that the experimenter can only control the rate at which the potential of one electrode varies with respect to the potential of the other electrode and (ii) its inability to selectively reduce/oxidize one species while more than one redox couple are present in the medium. In other words, the CB response is obtained through oxidation and reduction of whatever species which can undergo redox reactions more easily in both directions within the applied voltage window. However, by incorporating a reference electrode in CV, one can selectively reduce/oxidize the analyte of interest while keeping the other redox-active analytes in either their oxidized or reduced form(s).

The detection limit of cyclic biamperometry using interdigitated electrodes was calculated to be 2.6×10^{-7} M based on 3 standard deviations. This detection

limit was obtained using symmetric comb-shaped IDEs, where the total surface area of cathodes and anodes are equal, at equimolar concentrations of ferri and ferrocyanide. Potentially lower detection limit can be obtained by keeping the concentration of one redox species in excess and using asymmetrical IDEs where the surface area of cathodes and anodes are not equal to one another.

Preliminary results[1] show that this method can be applied to bioassays. For example, Figure 4.1 shows how CB can be implemented to monitor the activity of alkaline phosphatase. In this case, alkaline phosphatase dephosphorylates 1-naphthyl phosphate to produce 1-naphthol which in turn, reacts with ferricyanide to produce ferrocyanide as well as an organic oxidation product that precipitates in the medium. In this example, ferrocyanide was present in excess so that ferricyanide acts as the limiting species and the sole determinant of the biamperometric peak currents. While catalysis of the reaction by alkaline phosphatase proceeds, more and more 1-naphthol is produced that consumes ferricyanide. Consequently, the peak currents gradually decrease.

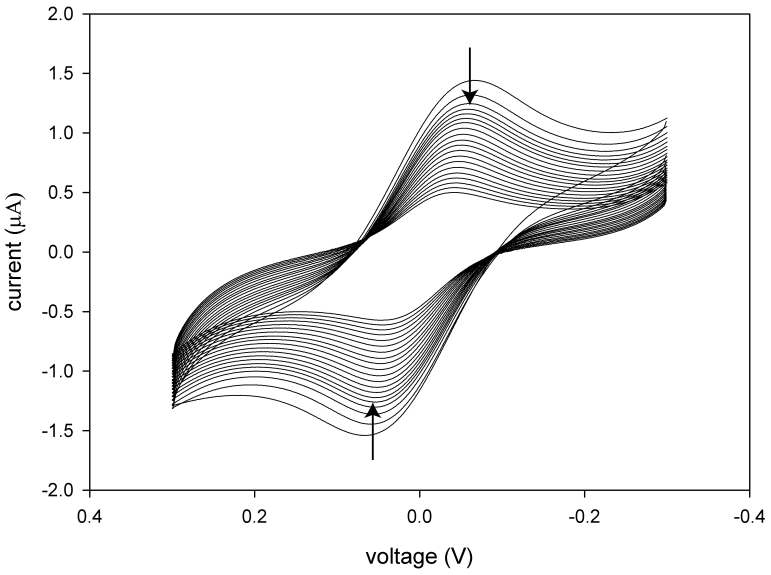

Figure 4.1: Monitoring the activity of alkaline phosphatase through dephosphorylation of 1-naphthyl phosphate. The product, 1-naphthol, is oxidized by ferricyanide to produce ferrocyanide. As the concentration of ferricyanide decreases in the medium, peak currents also decrease proportionally. The solution contains 3 μM shrimp alkaline phosphatase, 2.00 mM ferricyanide, excess ferrocyanide, 1.00 mM p-nitrophenyl phosphate, 1.00 M diethanolamine buffer (pH 9.7) with 15 mM KCl and 1.0 μM $MgCl_2$

Finally, much simpler electronic circuitry containing only a voltage source and a highly sensitive ammeter can potentially lead to more sensitive measurements by

[1]This experiment was carried out by Taras Rybak, one of our former group members and these unpublished results are included with his permission.

reducing the background noise.

Further work with this method could include applications to simple (e.g. single enzyme) and more complicated (e.g. whole cell) bioassays, and the applications of electrode-surface-immobilized biocatalysts for highly sensitive substrate biosensors. Also, by using IDEs with smaller dimensions than those studied in this thesis the detection of single enzyme molecules may be possible. For example, the turnover number of calf intestinal alkaline phosphatase has been reported to be 1.00×10^5 per molecule per minute at 31°C in 2.4 M diethanolamine buffer (pH 10.0) containing 57 μM $MgCl_2$ using p-nitrophenyl phosphate as the substrate.[28]

Assuming that each molecule of p-nitrophenol can reduce 3 molecules of ferricyanide, 3.00×10^5 molecules of ferrocyanide can be produced per molecule of alkaline phosphatase per minute. So, theoretically, in a solution containing 1 ALP molecule in 10 μL (the volume required to be put on the interdigitated electrodes), 3.00×10^6 molecules of ferrocyanide can be produced after 10 min incubation time. This would be equal to a 4.98×10^{-13} M ferrocyanide solution.

According to the Eq. 1-5, the current obtained using the smaller IDEs used introduced in this thesis with 5 μm gap and a surface area of $3.4_{75} \times 10^{-3}$ cm^2 is,[2]

$$I = \frac{nFADC}{d}$$

$$= \left(\frac{96487 \left(\frac{\mathrm{C}}{\mathrm{mole}}\right) 3.475 \times 10^{-3}(\mathrm{cm}^2) 6.50 \times 10^{-6} \left(\frac{\mathrm{cm}^2}{\mathrm{s}}\right) 4.98 \times 10^{-13} \left(\frac{\mathrm{mole}}{\mathrm{cm}^3}\right)}{5 \times 10^{-4}\mathrm{cm}} \right)$$

$$= 2.13 \times 10^{-12} \text{ A}$$

This current is measurable by highly sensitive ammeteres which are now commercially available. It is also possible to improve the current by designing a special IDE design (with $A_{W_2} > A_{W_1}$).

Finally. due to the lack of a reference electrode, cyclic biamperometry can be readily incorporated into instrumental array systems for parallel, high throughput measurements such as in a biamperometric microplate reader.

[2]Equation 1-5 was introduced for nano-fluidic interdigitated channels with 75 nm channel height however, here, it is assumed that this equation is applicable to interdigitated electrodes because the thickness of the gold electrodes used in this thesis is practically in the same order of magnitude as height of the nano-fluidic interdigitated channels.

References

[1] A. J. Bard, L. R. Faulkner, Electrochemical Methods, Fundamentals and Applications, Second Edition, 2001, John Wiley & Sons, Inc.

[2] P. T. Kissinger, W. R. Heineman, Laboratory Techniques in Electroanalytical Chemistry, Second Edition, 1999, Marcel Dekker Inc.

[3] G. S. Forbes, E. P. Bartlett, The Increase in the Oxidizing Potential of the Dichromate Ion on Platinum Caused by Certain Reducing Agents. An Improved Method for the Electrometric Titration of Ferrous Salts, Journal of the American Chemical Society, (1913), 35, 1527-38.

[4] V. Frantisek, K. Stulik, The determination of iron and aluminum in silicates by chelatometric titration combined with biamperometric indication, Acta Geologica et Geographica Universitatis Comenianae, Geologica, (1968), 15, 87-91.

[5] M. Jovanovic, B. Vucurovic, New methods for the determination of hydroxylammonium salts by neutralization. Proceeding in Analytical Chemistry Conference, 3rd (1970), 2, 191-7.

[6] M. L. Tsap, V. Y. Kisel, E. L. Panasenko, Determination of molybdenum in vegetable matter by a biampere-kinetic method. Vestnik Sel'skokhozyaistvennoi Nauki (Moscow) (1971), 16(1), 106-18.

[7] L. L. Jun, Q. F. Chen, H. Cheng, L. B. Yu, J. L. Wu, Determination of levodopa in pharmaceutical preparations by irreversible biamperometry. Chinese Chemical Letters (2008), 19(6), 703-706.

[8] J. C. Zhang, Y. N. Chen, L. L. Wang, Flow injection biamperometric analysis of uric acid. Fenxi Ceshi Xuebao (2007), 26(5), 718-721.

[9] C. Zhao, J. Song, J. Zhang, Flow injection biamperometry of pyrogallol compounds. Talanta (2003), 59(1), 19-26.

[10] S. Milardovic, I. Kerekovic, M. Nodilo, A novel biamperometric biosensor for urinary oxalate determination using flow-injection analysis. Talanta (2008), 77(1), 222-228.

[11] C. Zhao, J. Zhang, J. Song, Determination of L-cysteine in amino acid mixture and human urine by flow-injection analysis with a biamperometric detector, Analytical Chemistry, (2001), 297, 170-176.

[12] C. Zhao, J. F. Song, J. C. Zhang, Determination of total phenols in environmental waste water by flow-injection analysis with a biamperometric detector, Analytical and Bioanalytical Chemistry (2002), 374, 498-504.

[13] J. F. Song, J. Q. Chen, Flow-injection biamperometric direct determination of calcium dobesilate in irreversible couple system, Journal of Pharmaceutical and Biomedical Analysis, (2003), 33, 789-796.

[14] S. Milardovic, D. Ivekovic, V. Rumenjak, B. S. Grabaric, Use of DPPH/DPPH redox couple for biamperometric determination of antioxidant activity, Electroanalysis (2005), 17, 1847-1853.

[15] S. Milardovic, I. Kerekovic, R. Derrico, V. Rumenjak, A novel method for flow injection analysis of total antioxidant capacity using enzymatically produced $ABTS^+$ and biamperometric detector containing interdigitated electrode, Talanta (2007), 71, 213-220.

[16] A. J. Bard, L. R. Faulkner, Electrochemical Methods, Fundamentals and Applications, Second Edition, (2001), John Wiley & Sons, Inc. p655.

[17] E. D. Goluch, B. Wolfrum, P. S. Singh, M. A. G. Zevenbergen, S. G. Lemay, Redox cycling in nanofluidic channels using interdigitated electrodes. Analytical and Bioanalytical Chemistry (2009), 394(2), 447-456.

[18] J. Wang, Analytical Electrochemistry, 2^{nd} Ed. 2000 Wiley-VCH p.129

[19] O. Niwa, M. Morita, H. Tabei, Electrochemical behavior of reversible redox species at interdigitated array electrodes with different geometries : consideration of redox cycling and collection efficiency. Analytical Chemistry (1990), 62(5), 447-52.

[20] X. Yang, G. Zhang, The voltammetric performance of interdigitated electrodes with different electron-transfer rate constants. Sensors and Actuators, B: Chemical (2007), B126(2), 624-631.

[21] O. Niwa, M. Morita, H. Tabei, Highly selective electrochemical detection of dopamine using interdigitated array electrodes modified with Nafion/polyester ionomer layered film. Electroanalysis (1994), 6(3), 237-43.

[22] V. A. T. Dam, W. Olthuis, A. Van den Berg, Redox cycling with facing interdigitated array electrodes as a method for selective detection of redox species. Analyst (Cambridge, United Kingdom) (2007), 132(4), 365-370.

[23] R. N. Adams, Electrochemistry at solid electrodes, 1^{st} Ed. (1969) Marcel Dekker, Inc.

[24] Yim, Sung-Kun; Yun, Su-Jung; Yun, Chul-Ho. A continuous spectrophotometric assay for NADPH-cytochrome P450 reductase activity using 1,1-diphenyl-2-picrylhydrazyl. Journal of Biochemistry and Molecular Biology (2004), 37(5), 629-633.

[25] A. M. Alkilany, R. L. Frey, J. L. Ferry,C. J. Murphy, Gold Nanorods as Nanoadmicelles: 1-Naphthol Partitioning into a Nanorod-Bound Surfactant Bilayer, Langmuir (2008), 24, 10235-10239

[26] M. L. Mihailovic, Z. Cekovic, Oxidation and reduction of phenols, Part 1, Chapter 10, Edited by S. Patai Ed. Wiley & Sons Interscience, 1971, pp. 505-592.

[27] C. G. Haynes, A. H. Turner, William A. Waters, The oxidation of monohydric phenols by alkaline ferricyanide, Journal of Chemical Society, 1956, 2823-2831.

[28] D. B. Craig, J. C. Y. Wong, N. J. Dovichi, Detection of attomolar concentrations of alkaline phosphatase by capillary electrophoresis using laser-induced fluorescence detection, Analytical Chemistry, 1996, 68 (4), 697700.